Enhanced Coupling Structures for Tight Couplers and Wideband Filters

Cheng-Hsien Liang, Wei-Shin Chang, and Chi-Yang Chang, *Member, IEEE*

***Abstract*—Tightly coupled lines are difficult to realize on the conventional printed circuit board (PCB). This paper proposes two types of novel enhanced coupled-line structures appropriate for tightly coupled directional couplers and wideband filters. The proposed coupled-line structures both have a rectangular ground-plane aperture and two inserted signal strips in the aperture to increase the coupling strength significantly. No fine lines and narrow gaps are required so as to fit the conventional PCB fabrication process. More importantly, the proposed structures only need a single-layer substrate. To demonstrate the feasibility of the proposed structures, one 3-dB directional coupler and two four-pole Chebyshev filters with 0.05-dB equal-ripple bandwidths of 40% and 37% are designed and realized. The coupler and filters are fabricated on a PCB substrate with a dielectric constant of 3.58 and a thickness of 0.508 mm. Good agreement between measurements and simulations is observed.**

***Index Terms*—Coupled line, defected ground structure (DGS), directional coupler, microstrip line, parallel-coupled microstrip filter, wideband bandpass filter (BPF).**

I. Introduction

MODERN commercialized microwave subsystems commonly use a printed circuit board (PCB) as a substrate to implement circuits for lower cost. The minimum line width and gap spacing in the conventional PCB process are approximately 0.15 mm. On the other hand, most of the popularly used PCBs have low dielectric constants. It is inherently difficult to implement tightly coupled lines with low dielectric-constant substrates. Nevertheless, tightly coupled directional couplers (especially a 3-dB coupler) and wideband filters are essential components in modern wireless communication systems. Moreover, microstrip components are particularly important due to easy integration into the PCB. For the tight coupler and wideband filter design, strongly coupled microstrip lines [see Fig. 1(a)] are required.

Various approaches have been proposed to design tight couplers. The most famous one is the Lange coupler [1]–[3], which is used extensively in the monolithic microwave integrated circuit (MMIC). However, the line width and gap spacing for either a four- or six-line 3-dB Lange coupler will be far below the fabrication limitation of the PCB process if a common substrate (for example, a RO4003 substrate with a dielectric constant of 3.58 and a thickness of 0.508 mm) is used. The vertically installed planar (VIP) structure [4], [5] could fit the PCB process, but it needs some special tools to solder the vertical substrate. The multilayer structure [6]–[8] requires multilayer substrates. The floating-plate overlay structure [9] needs small, overlaid substrates. All the structures in [4]–[9] lead to higher fabrication costs compared to a single-layer substrate structure. A 3-dB coupler can be fabricated on a single-layer substrate with broadside-coupled structures employing coplanar waveguides (CPWs) [10], [11]. Nevertheless, these structures may have the input and output ports on different sides of the substrate and might be difficult to apply to wideband filter design. Since there must be ground plane metals on two sides of the top layer, filter topologies such as interdigital, combline, or hairpin filters are not suitable.

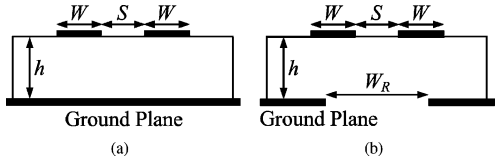

Fig. 1. Cross-sectional views of symmetric coupled microstrip lines. (a) Conventional. (b) Modified with the ground-plane aperture.

To design a microstrip, wideband, coupled-resonator bandpass filter (BPF) on the PCB, there are many published works. The ground plane aperture technique and the defected ground structure (DGS), as shown in Fig. 1(b), are commonly used to enhance the coupling [12]–[14]. In Fig. 1(b), the aperture width W_R varies according to the required coupling strength. Dual-plane and broadside-coupled structures [15]–[17] enable the stronger coupling, and filters with these structures inherently exhibit wideband characteristics. Other techniques, such as multilayer structures [9], [18], three-line microstrips [19], multimode resonators [20], [21], and the new coupling scheme in [22] are used to design wideband BPFs. However, the above-mentioned filters may be large, require multilayer technology, or have a narrow upper stopband. In [23], the interdigital coupling structure was used for coupling enhancement to design a small wideband BPF, but this structure is unable to realize a tight coupler. Thus, it is more appropriate to design a new coupling structure suitable for tight couplers, wideband filters, and other circuits that require strong coupling.

In this study, two types of microstrip, coupled-line structures with a rectangular ground-plane aperture and two inserted signal strips in the aperture are presented. Compared to the conventional coupled lines with or without the ground-plane aperture

Manuscript received October 04, 2010; accepted October 22, 2010. Date of publication December 17, 2010; date of current version March 16, 2011. This work was supported in part by the National Science Council (NSC), Taiwan, under Grant NSC 98-2221-E-009-034-MY3 and Grant NSC 99-2221-E-009-050-MY3.

The authors are with the Graduate Institute of Communication Engineering, National Chiao-Tung University, Hsinchu 300, Taiwan (e-mail: seaman.cm96g@g2.nctu.edu.tw; aa494412338@hotmail.com; mhchang@cc.nctu.edu.tw).

Color versions of one or more of the figures in this paper are available online at http://ieeexplore.ieee.org.

Digital Object Identifier 10.1109/TMTT.2010.2094202

0018-9480/$26.00 © 2010 IEEE

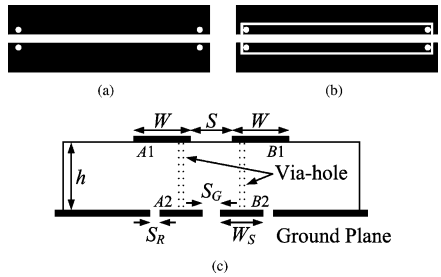

Fig. 2. Proposed coupled microstrip lines of type I. (a) Top view. (b) Bottom view. (c) Cross-sectional view.

shown in Fig. 1, the proposed ones have a much stronger coupling strength. Both proposed coupled-line structures have the advantages of process compatibility with the conventional PCB process, top-layer signal traces, and same-side input/output ports. A 3-dB directional coupler was designed and manufactured using the proposed method. The implemented coupler is compact and only has two-finger coupled lines. In addition, the new enhanced coupling structures are conveniently adopted in any part of the resonator where the strong coupling is required. Here, we use the proposed structures in the conventional $\lambda/4$ resonator to design wideband BPFs. The coupling strength between adjacent resonators is easily varied by adjusting the size of the ground-plane aperture and the width of inserted signal strips. Two compact, wideband BPFs were designed and fabricated. The implemented filters show that the proposed structures effectively solve the coupling strength problem of conventional microstrip resonators.

II. Proposed Coupled-Line Structures

A. Type I

Fig. 2 shows the top, bottom, and cross-sectional views of the proposed coupled microstrip lines of type I. The proposed structure, where there are two inserted signal strips in the ground plane, is basically an extension of the modified coupled lines shown in Fig. 1(b). Note that two via-holes are added on each end of the inserted signal strip on the bottom layer, penetrate through the substrate, and appear on both ends of each signal strip on the top layer. Therefore, the strip conductor $A1$ is connected to $A2$ and $B1$ is connected to $B2$. To separate the inserted signal strip from the microstrip ground plane on the bottom layer, there is a narrow gap between them. In the proposed structure, the width of two microstrip lines on the top layer is W and the spacing between them is S. The width of two inserted signal strips with a spacing S_G on the bottom layer is W_S. The spacing between the inserted signal strips and the microstrip ground plane is S_R. Accordingly, the width of the ground-plane aperture is $W_R = 2 \times (W_S + S_R) + S_G$. In the quasi-static analysis, the coupling strength of the symmetric coupled lines is determined by the even- and odd-mode capacitances C_e and C_o or by the even- and odd-mode impedances Z_e and Z_o. The voltage coupling factor C for the coupled lines is given by [3]

$$C = \frac{Z_e - Z_o}{Z_e + Z_o}. \tag{1}$$

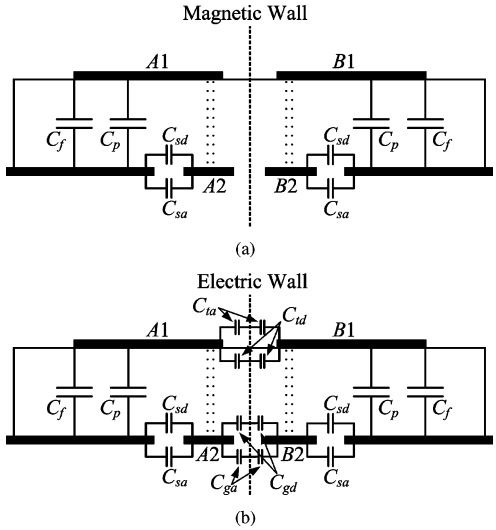

Fig. 3. Quasi-TEM modes of the proposed coupled microstrip lines (type I). (a) Even mode. (b) Odd mode.

Consequently, the larger the difference between the even- and odd-mode impedances is, the stronger the coupling between the lines will be.

Fig. 3 shows the even- and odd-mode excitations of the proposed coupled-line structure. For the even-mode excitation shown in Fig. 3(a), the normal component of the electric field at the symmetry plane is zero, which results in a magnetic wall. On the other hand, under the odd-mode excitation, the symmetry plane behaves like an electric wall, as indicated in Fig. 3(b). In Fig. 3, C_p denotes the parallel-plate capacitance located vertically between the signal and ground planes. C_f is the fringe capacitance from the edge of an uncoupled microstrip line. C_{sa} and C_{sd} represent the fringe capacitances across the gap between the inserted signal strip and the ground plane in the air and dielectric regions, respectively. For the odd-mode excitation in Fig. 3(b), C_{ta} and C_{td} are the fringe capacitances across the coupling gap in the air and dielectric regions, respectively, on the top layer, whereas C_{ga} and C_{gd} are those on the bottom layer. Therefore, the even- and odd-mode capacitances (C_e, C_o) of either of the coupled lines are given by

$$C_e = C_f + C_p + C_{sa} + C_{sd} \tag{2}$$

$$C_o = C_f + C_p + C_{sa} + C_{sd} + C_{ta} + C_{td} + C_{ga} + C_{gd}. \tag{3}$$

To compare the characteristics of the conventional and proposed coupled lines shown in Figs. 1 and 2, first of all, it is necessary to obtain the even- and odd-mode impedances of coupled lines. We first perform the full-wave electromagnetic (EM) simulation for coupled lines by using Sonnet software [24], and then load the four-port S-parameter file in AWR Microwave Office [25] to obtain the even- and odd-mode impedances. During the simulation, a lossless metal is assumed, and a substrate with a dielectric constant $\epsilon_r = 3.58$ and a thickness $h = 0.508$ mm is used. Since the capability of the available fabrication process is taken into account, each via-hole is 0.3 mm in diameter, and the minimum line width and gap spacing are limited to be 0.15 mm. Since there are too many physical parameters in the proposed structure, the dimensions S, S_G, and S_R are fixed at 0.15 mm.

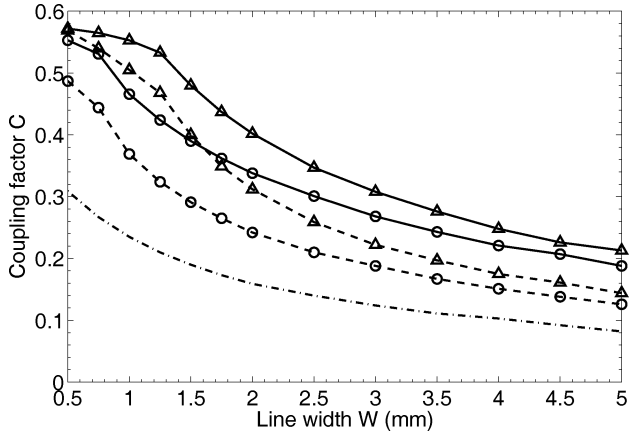

Fig. 4. Coupling factor C versus microstrip-line width W for two aperture sizes $W_R = 1.65$ mm (circle ◯) and 2.85 mm (triangle △). Conventional: dashed–dotted line. Modified with the ground-plane aperture: dashed line. Proposed: solid line.

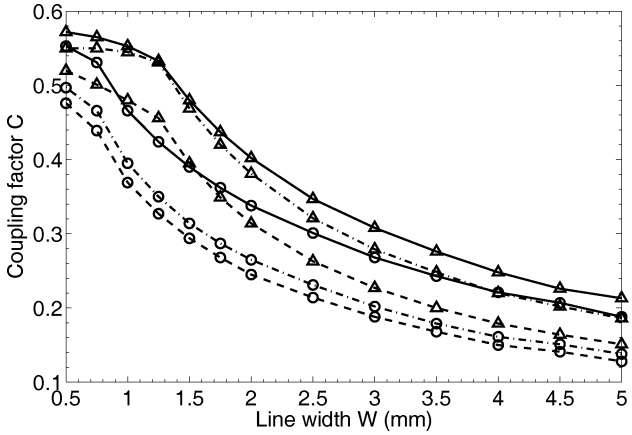

Fig. 5. Comparison of the coupling factor C for three different coupled lines with two aperture sizes $W_R = 1.65$ mm (circle ◯) and 2.85 mm (triangle △). Structure in [26]: dashed–dotted line. Proposed without via-holes: dashed line. Proposed with via-holes: solid line.

Fig. 4 plots the coupling factor C versus microstrip line width W for two different aperture sizes $W_R = 1.65$ mm and 2.85 mm, corresponding to $W_S = 0.6$ mm and 1.2 mm. The lengths of the coupled lines and the ground-plane aperture are 33.75 and 33.15 mm, respectively. The figure shows that as W varies from 0.5 to 5 mm, the proposed structure always has the largest coupling factor compared to the conventional parallel coupled lines with or without the ground-plane aperture under the same physical dimensions. Furthermore, the wider the width W_R of the ground-plane aperture is, the larger the coupling factor C will be. The increasing percentage of the coupling factor is especially larger for wide lines. This property is very advantageous since, for the filter application, it is very difficult to obtain strong coupling for wide lines.

To explain the mechanism behind the proposed structure in Fig. 4, first, consider the conventional coupled lines with and without the ground-plane aperture, as shown in Fig. 1. For the coupled lines without the ground-plane aperture, the even-mode impedance Z_e is larger than the odd-mode impedance Z_o since the even-mode capacitance C_e is smaller than the odd-mode capacitance C_o. For the coupled lines with the ground-plane aperture in Fig. 1(b), the decreasing percentage of C_e is greater than that of C_o owing to the ground-plane aperture. For this reason, the increasing percentage of Z_e is greater than that of Z_o, which results in a stronger coupling compared to the conventional structure in Fig. 1(a). On the basis of the structure in Fig. 1(b), now consider the proposed structure shown in Fig. 2 and the even- and odd-mode excitations given in Fig. 3. It is seen that the inserted signal strip in the ground-plane aperture increases C_e and C_o simultaneously due to capacitances C_{sa} and C_{sd} in both even- and odd-mode excitations. As the width W_S of the inserted signal strip increases, both capacitances C_e and C_o increase due to the increases of C_{sa} and C_{sd}. Additionally, the inserted signal strip introduces C_{ga} and C_{gd} in the odd-mode excitation. Thus, the increasing percentage of C_o is much greater than that of C_e. In other words, the proposed structure decreases Z_e and Z_o at the same time, and the decreasing percentage of Z_e is much smaller than that of Z_o. This method effectively enhances the coupling strength compared to the structure in Fig. 1(b).

It is interesting to compare the proposed coupled lines with and without via-holes and the coupled-line structure with a floating ground-plane conductor in [26]. Here, the dimensions in Fig. 4 are used as an example so that $W_R = 1.65$ mm and 2.85 mm correspond to the width of the floating ground-plane conductor 1.35 and 2.55 mm in [26], respectively. Since the coupling enhancement is concerned in this study, Fig. 5 shows the coupling factor C for these three structures. As shown in the figure, the structure in Fig. 2 always has the largest coupling factor, and via-holes are necessary for strong coupling. The via-holes in the proposed structure have an extremely small size and are primarily used for maintaining equal potentials on the top and bottom signal strips. In other words, they are not used to connect the signal strip to the ground plane. Accordingly, the current on the coupled lines is mainly along the longitudinal direction so that the inductive effect of via-holes is not severe and can be neglected.

B. Type II

Fig. 6 depicts the top, bottom, and cross-sectional views of the proposed coupled microstrip lines of type II. In comparison with type I, type II has the same cross-sectional profile, except that the signal strips on the top layer are cross-connected to the inserted signal strips in the ground plane. Therefore, in Fig. 6(b) and (c), the strip conductor $A1$ is connected to $A2$ and $B1$ is connected to $B2$. Although two pairs of via-holes are not placed symmetrically on both sides with respect to the central vertical plane, the even- and odd-mode excitations are still applied since the via-holes are very small compared to the whole circuit. The even- and odd-mode excitations of type II are shown in Fig. 7. Under the same physical dimensions, the even-mode excitation in Fig. 7(a) is the same as that in Fig. 3(a) so that this structure has little influence on the even-mode impedance Z_e of type I. However, comparing the odd-mode excitations in Figs. 3(b) and 7(b), this structure further decreases the odd-mode impedance Z_o of type I due to additional capacitance C_s. Thereby, types I and II have nearly the same even-mode impedance, whereas type II has a much smaller odd-mode impedance compared to type I. As a result, the coupling factor of type II is larger than that of type I. Take

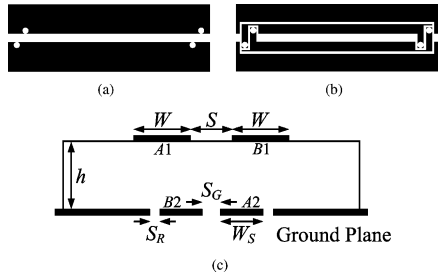

Fig. 6. Proposed coupled microstrip lines of type II. (a) Top view. (b) Bottom view. (c) Cross-sectional view.

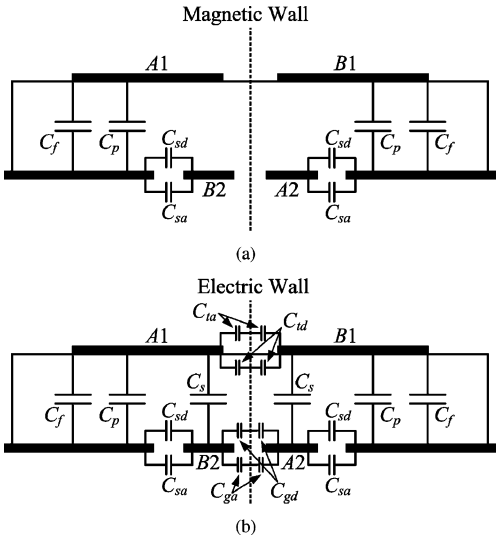

Fig. 7. Quasi-TEM modes of the proposed coupled microstrip lines (type II). (a) Even mode. (b) Odd mode.

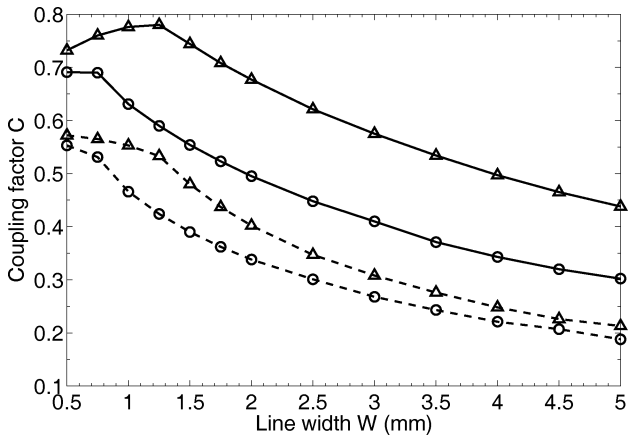

Fig. 8. Comparison of the coupling factor C versus microstrip linewidth W for types I (dashed line) and II (solid line) with two aperture sizes $W_R = 1.65$ mm (circle ◯) and 2.85 mm (triangle △).

the dimensions given in Fig. 4 as an example. Fig. 8 compares the coupling factor C versus microstrip line width W for types I and II to verify that type II has a much stronger coupling strength than type I.

III. Tight Coupler and Wideband Filter Design

To demonstrate the proposed coupling structures, one 3-dB directional coupler and two compact wideband BPFs were designed and implemented. All circuits were fabricated on the Rogers RO4003 substrate with a dielectric constant of 3.58, a loss tangent of 0.0021, and a thickness of 0.508 mm. Each via-hole has a diameter of 0.3 mm. The commercial full-wave EM simulation software Sonnet [24] was used to perform the simulation. Since there is a conducting box in Sonnet, the measurements of all circuits with attached standard subminiature A (SMA) connectors were carried out in a shielding box using an Agilent 8720ES network analyzer.

A. 3-dB Directional Coupler

To realize a tight coupler, the proposed structure of type II [see Fig. 6] is chosen. Fig. 9 plots the even- and odd-mode impedances versus normalized widths W/h (from 0.6 to 1.5) and W_S/h (from 0.3 to 1.6). Since there are many physical parameters in the proposed structure, we set $S/h = S_G/h = 0.3$ in Fig. 9(a) and (b) and $S/h = S_G/h = 0.6$ in Fig. 9(c) for easy comparison between parameters. Accordingly, the normalized ground-plane aperture width $W_R/h = 4.1$ and 4.7 in Fig. 9(a) and (b) correspond to $(W_S + S_R)/h = 1.9$ and 2.2, respectively, and $W_R/h = 4.4$ in Fig. 9(c) corresponds to $(W_S + S_R)/h = 1.9$. The figures show that both Z_e and Z_o decrease as W/h and W_S/h increase. Comparing Fig. 9(a) and (b), as W_R/h varies from 4.1 to 4.7, Z_e increases, whereas Z_o remains almost unchanged. From Fig. 9(a) and (c), as S/h and S_G/h increase from 0.3 to 0.6, Z_o increases, whereas Z_e remains almost the same. Thus, in the design process, we first determine W/h, W_S/h, and S_R/h according to Z_e, and then choose S/h and S_G/h for Z_o. In addition, Fig. 9 gives the variations of the even- and odd-mode effective dielectric constants ϵ_{ree} and ϵ_{reo}. The linear interpolation method is applied to estimate the even- and odd-mode effective dielectric constants owing to their small variations.

In this study, the coupler with a 3 ± 0.5-dB coupling factor was designed at the center frequency of 1.5 GHz. The corresponding even- and odd-mode impedances are $Z_e = 132.3\ \Omega$ and $Z_o = 18.9\ \Omega$. On the basis of the analytical results and the design curves presented in Fig. 9(a)–(c), Fig. 10 depicts the top and bottom layouts of the directional coupler along with its physical dimensions. Note that two additional via-holes are added on the middle of the coupler to eliminate the resonance. The two additional via-holes have little effect on the even- and odd-mode impedances and the coupling factor since they are very small compared to the whole circuit.

Fig. 11 displays the photograph of the fabricated coupler. The overall size of the coupler is 9.85 mm × 35.95 mm. Fig. 12 shows the simulated and measured responses. The measured results show that the coupling strength is 2.671 dB at the center frequency. The amplitude difference between port 2 (coupled port) and port 3 (through port) is less than 1 dB over the frequency range of 0.874–2.124 GHz, corresponding to a fractional bandwidth of 83.3%. The phase difference between the through and coupled ports is 89.61° at the center frequency and remains $90 \pm 1.5°$ from 0.1 to 2.138 GHz. The return loss and isolation are better than 18.7 and 17.4 dB in the operating band, respectively.

To show the sensitivity to fabrication tolerances for the proposed coupled-line structure, we modify the mask during the fabrication process because PCB factories cannot change their processing parameters to match our study. Fig. 13 presents

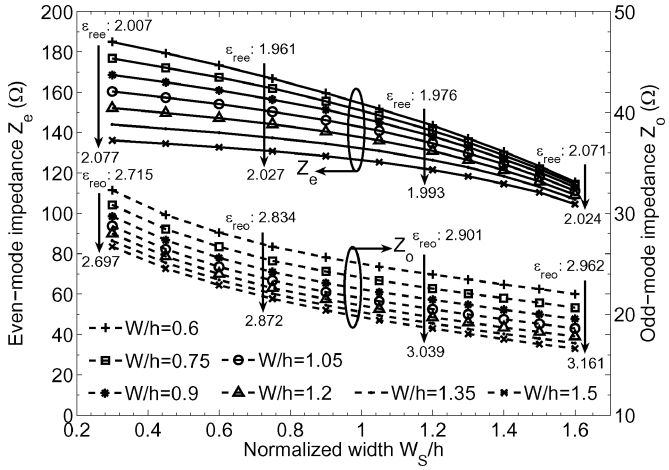

(a)

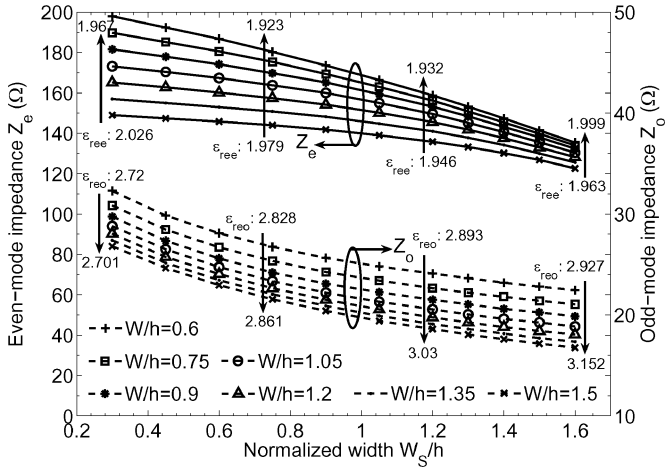

(b)

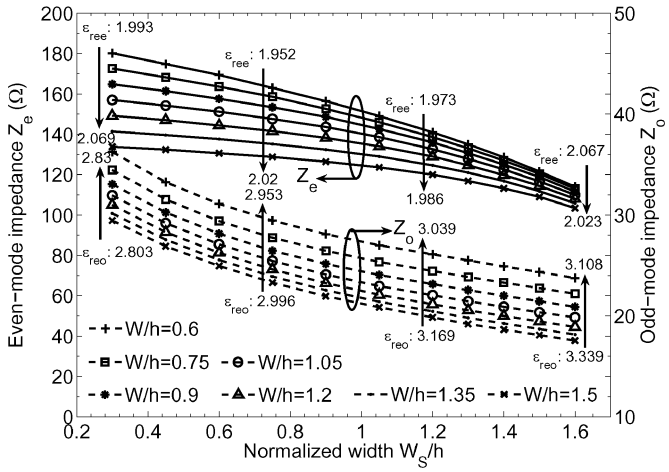

(c)

Fig. 9. Even- and odd-mode impedances (Z_e, Z_o) and effective dielectric constants (ϵ_{ree}, ϵ_{reo}) versus normalized values $W/h, W_R/h, W_S/h, S/h, S_G/h$, and S_R/h. (a) $W_R/h = 4.1$, $S/h = S_G/h = 0.3$, and $(W_S + S_R)/h = 1.9$. (b) $W_R/h = 4.7$, $S/h = S_G/h = 0.3$, and $(W_S + S_R)/h = 2.2$. (c) $W_R/h = 4.4$, $S/h = S_G/h = 0.6$, and $(W_S + S_R)/h = 1.9$.

the measured responses of the proposed 3-dB coupler versus etching error, i.e., from over-etching 0.05 mm (2 mil) to under-etching 0.025 mm (1 mil), to demonstrate its sensitivity. Only the insertion losses for the through port and the coupled port are shown for clarity. It is seen that the coupler is insensitive to manufacturing inaccuracies.

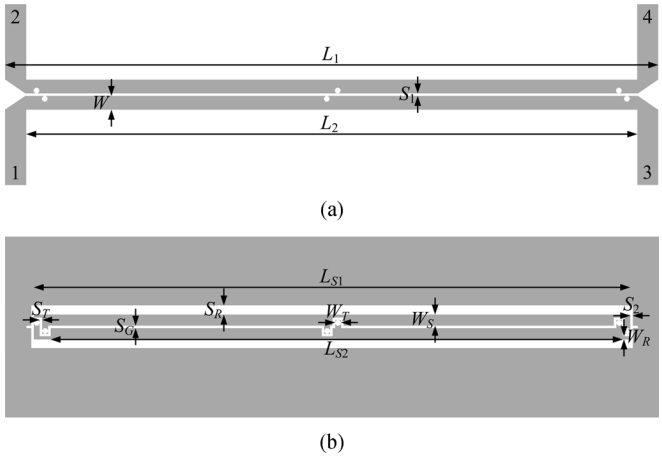

Fig. 10. Configuration of the proposed 3-dB coupler. (a) Top-layer layout. (b) Bottom-layer layout. Coupler dimensions: $L_1 = 35.95$ mm, $L_2 = 33.75$ mm, $L_{S1} = 32.85$ mm, $L_{S2} = 31.5$ mm, $S_1 = S_2 = S_T = S_G = 0.15$ mm, $S_R = 0.5$ mm, $W = 0.75$ mm, $W_S = 0.6$ mm, $W_T = 0.3$ mm, and $W_R = 0.15$ mm .

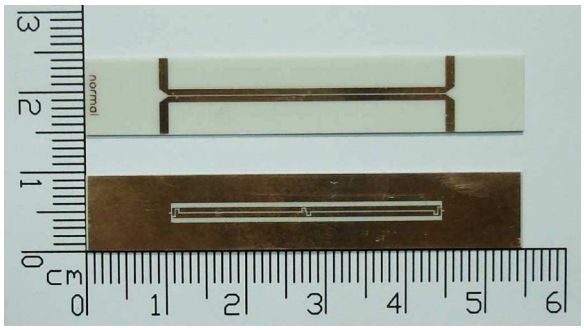

Fig. 11. Top view and bottom view of the fabricated coupler.

B. Wideband Quarter-Wavelength Parallel-Coupled Filter

Since a $\lambda/4$ resonator has a smaller size and fewer spurious modes than a $\lambda/2$ resonator, it is suitable for microstrip filters. The $\lambda/4$ parallel-coupled filter presented in [27] was adopted to design a four-pole Chebyshev filter with a passband ripple of 0.05 dB, a center frequency (f_0) of 1.5 GHz, and a fractional bandwidth of 40%. According to the analysis and design process in [27], the initial even- and odd-mode impedances of the coupling sections are $Z_e = 72.0728\,\Omega$ and $Z_o = 38.7455\,\Omega$. Since the formulas in [27] are suitable for narrowband filters, the developed filter should be fine tuned after the first design phase. Finally, the even- and odd-mode impedances of the coupling sections are $Z_e = 72.4\,\Omega$ and $Z_o = 38.8\,\Omega$. However, in this example, the spacing of the conventional parallel coupled lines is only 0.075 mm (i.e., smaller than 0.15 mm), which is beyond the fabrication capability. Hence, the proposed structure of type I [see Fig. 2] is used to obtain enough coupling.

Fig. 14 plots the even- and odd-mode impedances versus normalized widths W/h (from 1.4 to 2.6) and W_S/h (from 0.3 to 1.2), together with the variations of the even- and odd-mode effective dielectric constants. For easy comparison between parameters, we set $S/h = S_G/h = 0.5$ in Fig. 14(a) and (b)

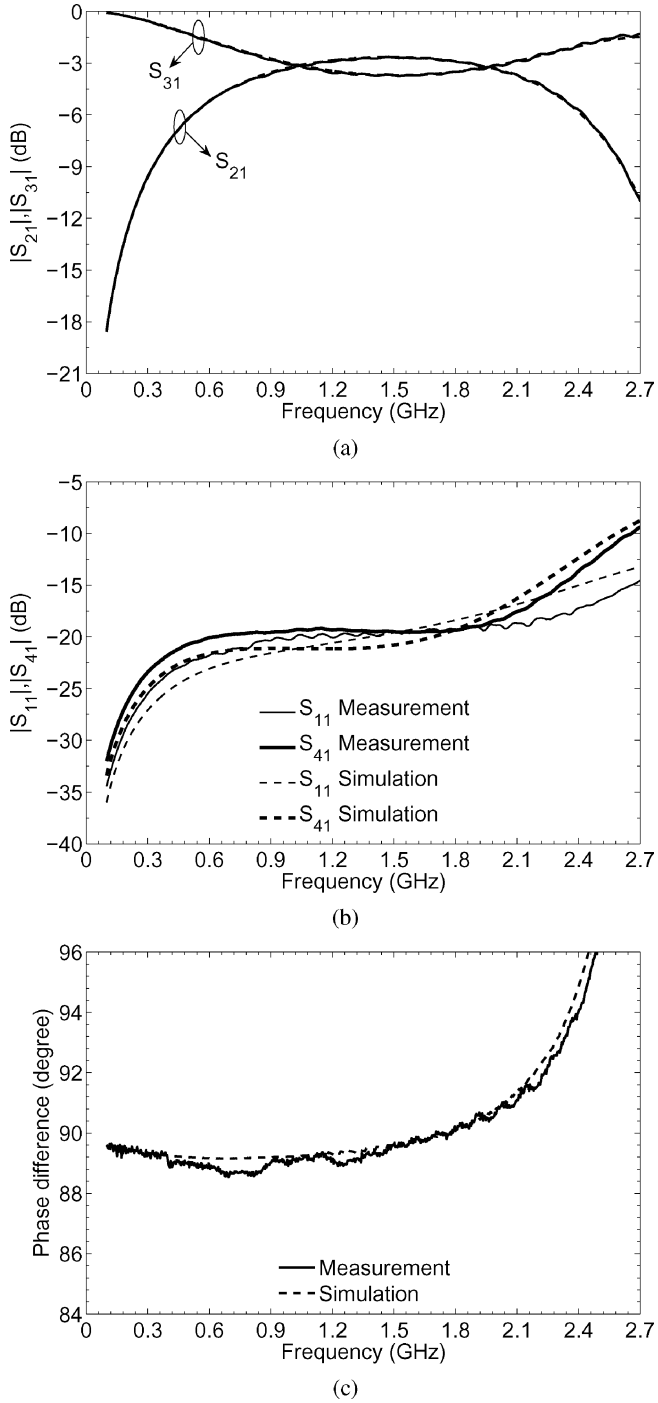

Fig. 12. Simulated (dashed line) and measured (solid line) results of the coupler. (a) Insertion losses $|S_{21}|$ and $|S_{31}|$. (b) Return loss $|S_{11}|$ and isolation $|S_{41}|$. (c) Phase difference between the through and coupled ports.

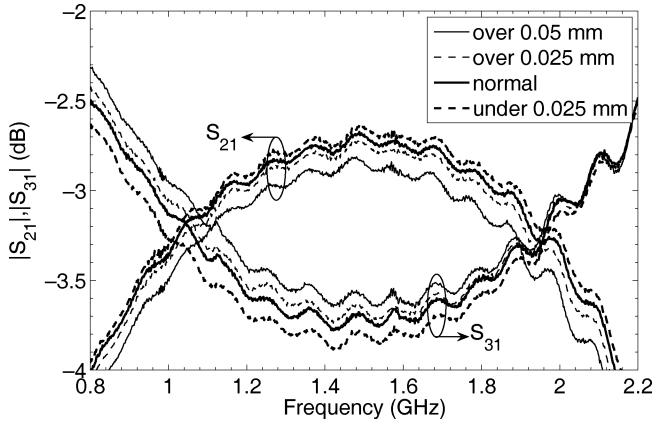

Fig. 13. Measured sensitivity to etching tolerances for the proposed 3-dB coupler (over: over-etching; under: under-etching).

and $S/h = S_G/h = 1.1$ in Fig. 14(c). Therefore, the normalized ground-plane aperture width $W_R/h = 3.5$ and 4.1 in Fig. 14(a) and (b) correspond to $(W_S + S_R)/h = 1.5$ and 1.8, respectively, and $W_R/h = 4.1$ in Fig. 14(c) corresponds to $(W_S + S_R)/h = 1.5$. As shown in the figure, both Z_e and Z_o decrease as W/h and W_S/h increase. From Fig. 14(a) and (b), as W_R/h varies from 3.5 to 4.1, Z_e increases obviously while Z_o increases slightly. Comparing Fig. 14(a) and (c), as S/h and S_G/h increase from 0.5 to 1.1, Z_o increases, whereas Z_e remains almost the same. On the basis of the above discussion, we first choose W/h, W_S/h, and S_R/h for Z_e, and then determine S/h and S_G/h according to Z_o. The even- and odd-mode effective dielectric constants are estimated using the linear interpolation method.

Once the even- and odd-mode impedances are determined, the dimensions of the coupling sections can be obtained using the design charts in Fig. 14. The physical layout and dimensions of the $\lambda/4$ parallel-coupled filter are shown in Fig. 15. Again, two additional via-holes are added on the middle of each coupling section to eliminate the resonance. Fig. 16 shows a photograph of the fabricated filter. The size of the filter is 55.8 mm $\times$ 4.3 mm, which is $0.4801\lambda_g \times 0.037\lambda_g$, where λ_g is the guided wavelength of the 50-Ω line on the substrate at the center frequency. The simulated and measured responses of the filter are presented in Fig. 17. The measured results show that the filter has a center frequency of 1.519 GHz. The measured 3-dB fractional bandwidth is 49.11% from 1.18 to 1.926 GHz. The filter has a minimum insertion loss of 0.5934 dB and a return loss better than 18.1 dB within the passband. The maximum passband group delay variation is 1.5 ns. The first spurious frequency is at 4.176 GHz ($= 2.75f_0$), and the rejection level is better than -20 dB from 2.381 to 4.109 GHz.

Fig. 18 presents the measured responses of the $\lambda/4$ parallel-coupled filter versus etching error, i.e., from over-etching 0.05 mm (2 mil) to under-etching 0.025 mm (1 mil). In spite of inaccurate fabrication, the center frequency and the bandwidth are almost unchanged. The passband return losses for all cases are better than 14.8 dB. Hence, the filter is insensitive to fabrication tolerances.

C. Wideband Quarter-Wavelength Hairpin Filter

The proposed coupling structures are easily incorporated in any part of the resonator where the strong coupling is needed. Fig. 19 depicts the top and bottom layouts of the folded microstrip $\lambda/4$ resonator with the proposed type I structure. Here, the resonator is folded in a hairpin shape in order to apply the electric and magnetic couplings easily. In comparison with the conventional $\lambda/4$ hairpin structure, the proposed one has an inserted signal strip in the ground plane along the edge of the open-end section of the resonator. The resonator has a top linewidth of W, and the width of the inserted signal strip in

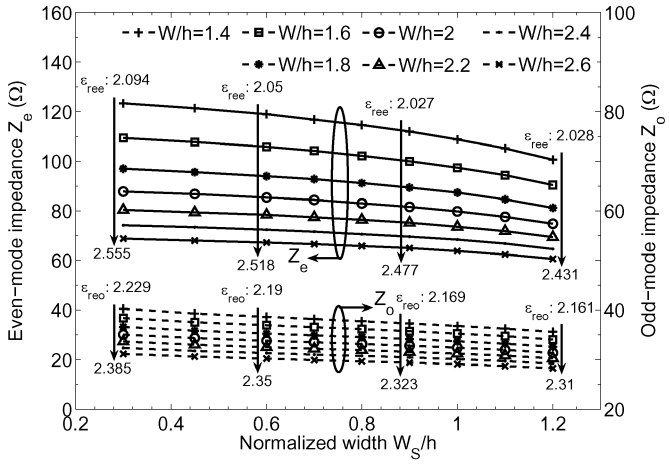

(a)

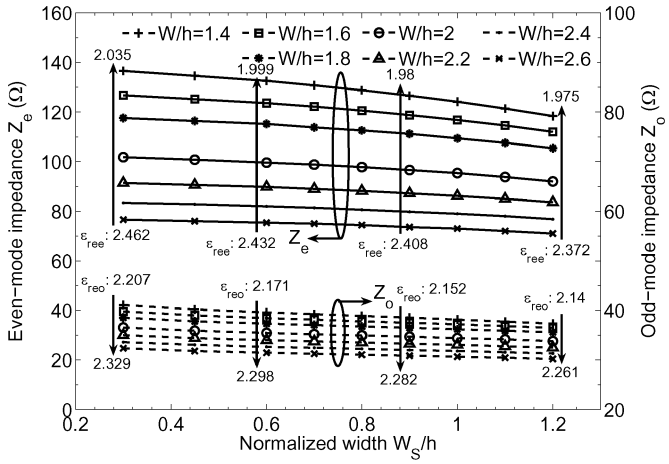

(b)

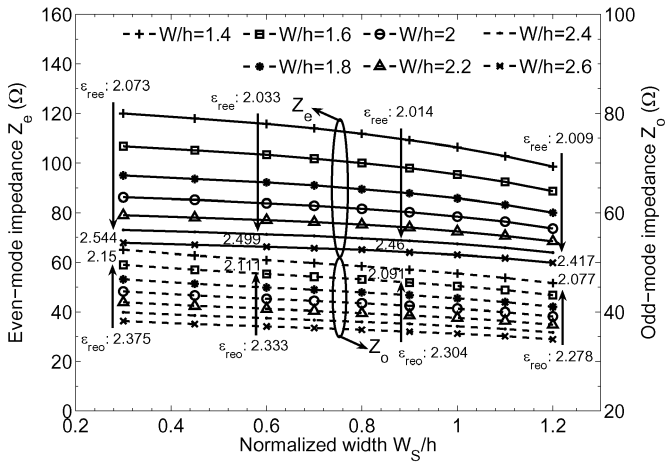

(c)

Fig. 14. Even- and odd-mode impedances (Z_e, Z_o) and effective dielectric constants (ϵ_{ree}, ϵ_{reo}) versus normalized values W/h, W_R/h, W_S/h, S/h, S_G/h, and S_R/h. (a) $W_R/h = 3.5$, $S/h = S_G/h = 0.5$, and $(W_S + S_R)/h = 1.5$. (b) $W_R/h = 4.1$, $S/h = S_G/h = 0.5$, and $(W_S + S_R)/h = 1.8$. (c) $W_R/h = 4.1$, $S/h = S_G/h = 1.1$, and $(W_S + S_R)/h = 1.5$.

the ground plane is W_S. The spacing between the inserted signal strip and the microstrip ground plane is S_R. The length of the inserted signal strip is L_S, and the total physical length of the resonator is $2 \times L_1 + L_2$. Since, in this example, the

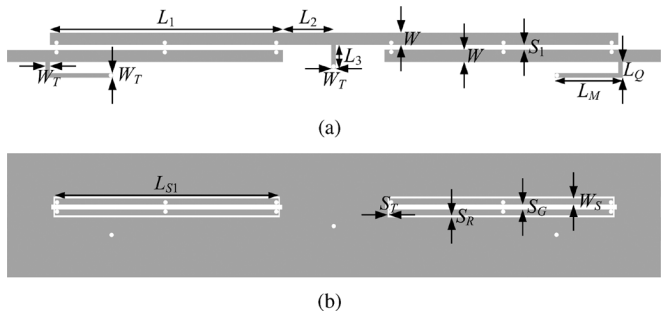

Fig. 15. Configuration of the four-pole $\lambda/4$ parallel-coupled filter. (a) Top-layer layout. (b) Bottom-layer layout. Filter dimensions: $L_1 = 22.8$ mm, $L_2 = 4.8$ mm, $L_3 = 2.35$ mm, $L_Q = 1.55$ mm, $L_M = 6.55$ mm, $L_{S1} = 21.9$ mm, $S_1 = S_G = 0.55$ mm, $S_T = 0.15$ mm, $S_R = 0.25$ mm, $W = 1.1$ mm, $W_S = 0.5$ mm, and $W_T = 0.3$ mm.

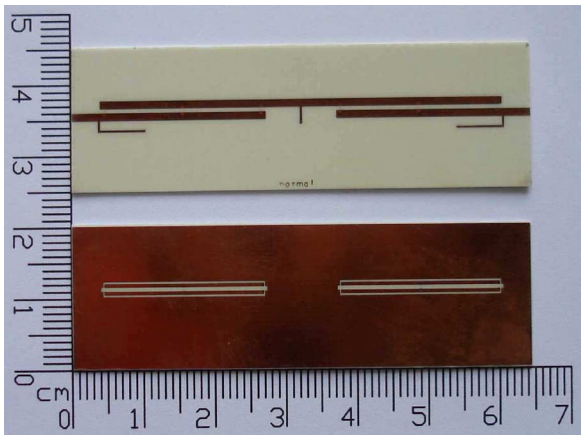

Fig. 16. Top view and bottom view of the fabricated $\lambda/4$ parallel-coupled filter.

length of the coupling section and the width of the resonator are arbitrarily chosen, the design procedure is conveniently based on the coupling coefficient k and the external quality factor Q_{ext} [28]. In the design process, we first fix W and S_R, and then adjust W_S iteratively to assure that the required coupling coefficient can be achieved for the minimum allowable spacing between resonators.

The designed four-pole $\lambda/4$ hairpin filter is a Chebyshev filter with a passband ripple of 0.05 dB, a center frequency (f_0) of 1.4 GHz, and a fractional bandwidth of 37%. According to the specifications, $Q_{\text{ext}} = 2.5913$, $k_{12} = k_{34} = 0.3318$, and $k_{23} = 0.2562$. The resonator dimensions are determined as follows: $L_2 = 2.5$ mm, $W = 0.75$ mm, $W_S = 0.3$ mm, and $S_R = 0.15$ mm.

For the resonator dimensions listed above, Fig. 20 plots the two basic coupling structures and the design curves for the proposed $\lambda/4$ hairpin filter. There are two kinds of couplings involved in the filter. At resonance, each of the $\lambda/4$ resonators has the maximum electric fringe fields near the open end and the maximum magnetic fringe fields around the short end. Hence, Fig. 20(a) is for the electric coupling and Fig. 20(b) is for the magnetic coupling. The proposed type I structure forms a strong capacitive coupling between resonators where the coupling strength is determined by the widths W and W_S and the spacings S and S_R. The strong magnetic coupling is realized by a common transmission line connected to ground.

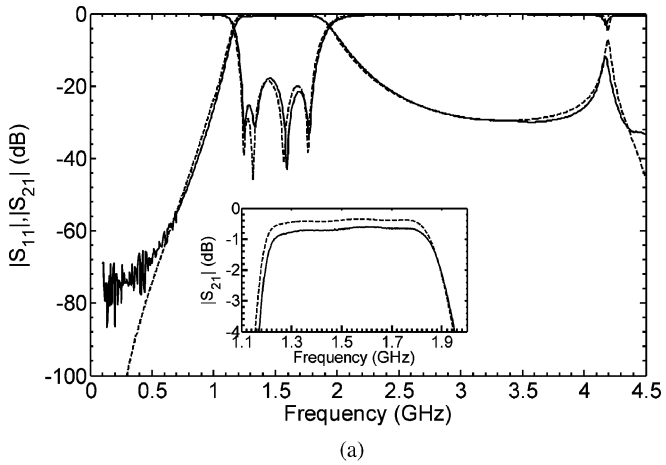

(a)

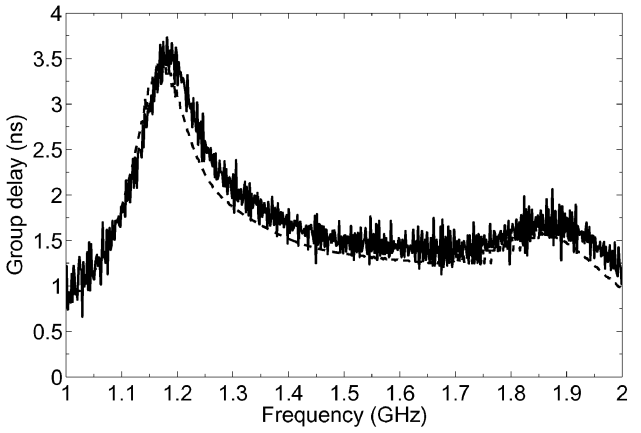

(b)

Fig. 17. Simulated (dashed line) and measured (solid line) results of the $\lambda/4$ parallel-coupled filter. (a) Scattering parameters. (b) Passband group delay.

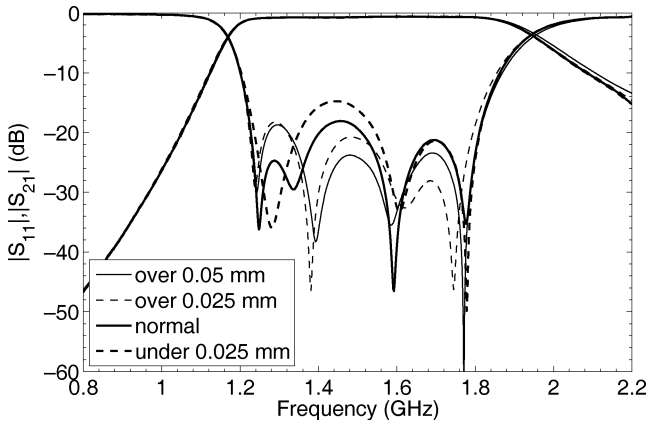

Fig. 18. Measured sensitivity to etching tolerances for the $\lambda/4$ parallel-coupled filter (over: over-etching; under: under-etching).

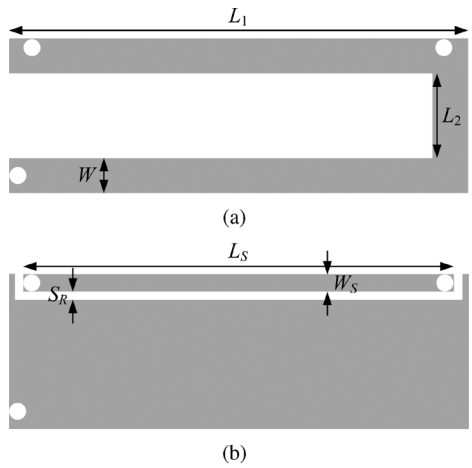

Fig. 19. Proposed $\lambda/4$ hairpin resonator. (a) Top view. (b) Bottom view.

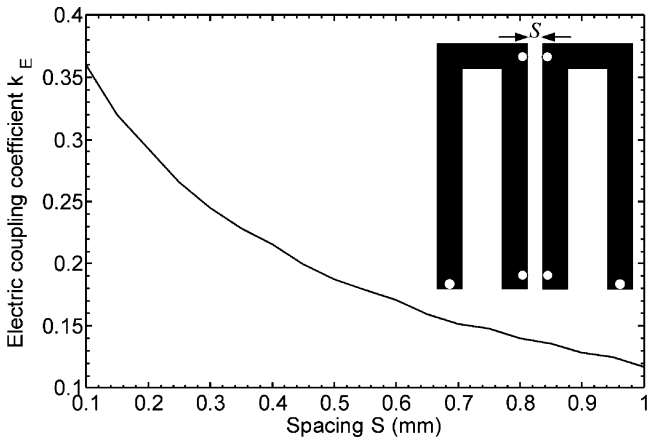

(a)

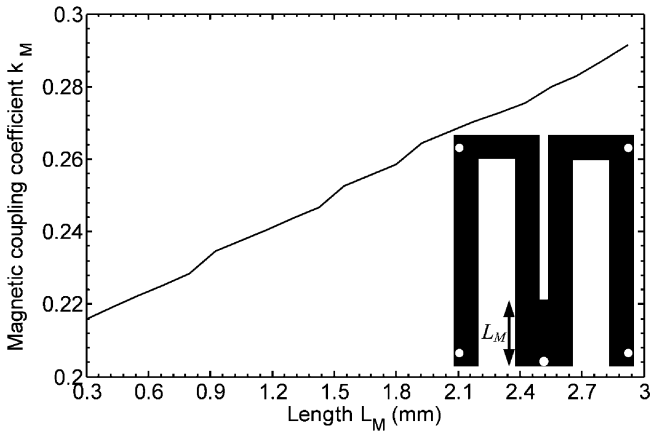

(b)

Fig. 20. Coupling structures and design curves for the proposed $\lambda/4$ hairpin filter. (a) Electric coupling and (b) Magnetic coupling.

The coupling strength is adjusted by the length L_M of the common short-circuited stub.

Fig. 21 depicts the physical layout and dimensions of the $\lambda/4$ hairpin filter. Here, we number these four resonators as 1–4 from left to right. The coupling k_{23} is magnetic, whereas k_{12} and k_{34} are electric. A tapped-line input/output structure is used for the external coupling since it is space saving and easy to design. The tap position L_Q is chosen to match the Q_{ext} value for the 50-Ω source/load impedance.

Fig. 22 shows a photograph of the fabricated $\lambda/4$ hairpin filter with a size of 16.45 mm $\times$ 15.5 mm, i.e., $0.1313\lambda_g \times 0.1237\lambda_g$. Fig. 23 illustrates the simulated and measured responses. The measured results show that the filter has a center frequency of 1.409 GHz. The measured 3-dB fractional bandwidth is 47.84%

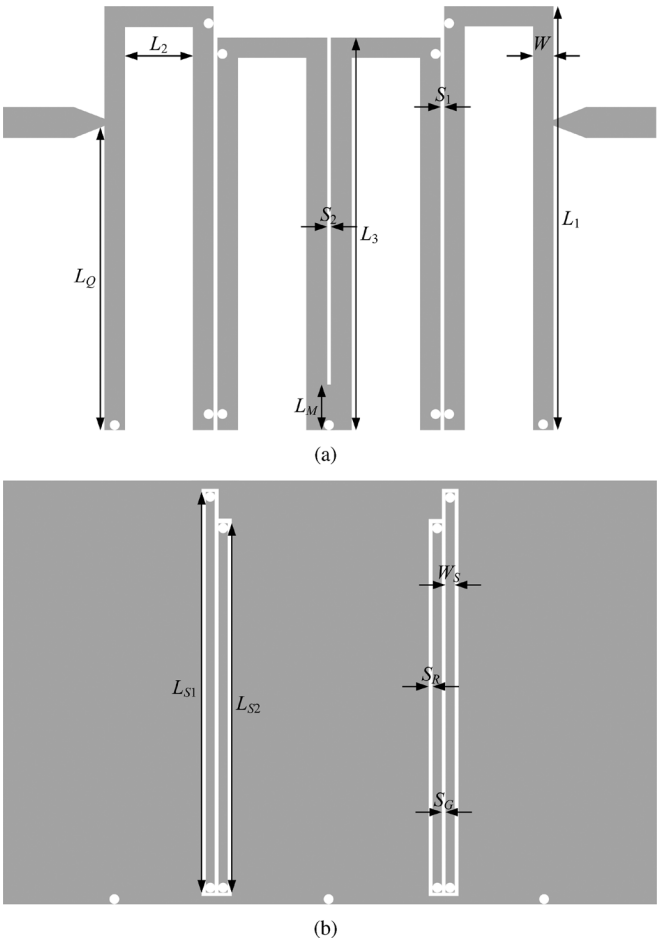

Fig. 21. Configuration of the proposed four-pole $\lambda/4$ hairpin filter. (a) Top-layer layout. (b) Bottom-layer layout. Filter dimensions: $L_1 = 15.5$ mm, $L_2 = 2.5$ mm, $L_3 = 14.35$ mm, $L_Q = 11.1$ mm, $L_M = 1.65$ mm, $L_{S1} = 14.6$ mm, $L_{S2} = 13.45$ mm, $S_1 = S_2 = S_R = S_G = 0.15$ mm, $W = 0.75$ mm, and $W_S = 0.3$ mm.

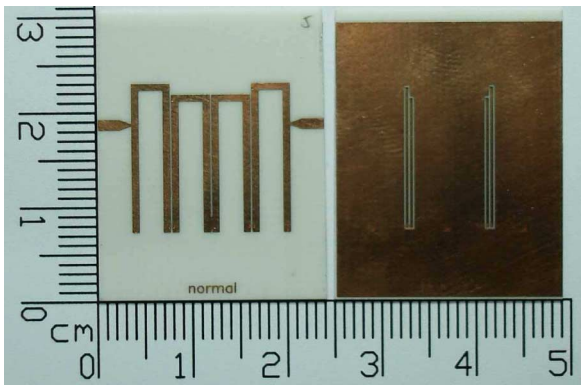

Fig. 22. (*left*) Top view and (*right*) bottom view of the fabricated $\lambda/4$ hairpin filter.

from 1.077 to 1.751 GHz. Within the passband, the minimum insertion loss is 0.6526 dB, and the return loss is better than 14.2 dB. The maximum passband group delay variation is 1.5 ns. The first spurious response is at 4.522 GHz ($= 3.21 f_0$), and the rejection level is better than -20 dB from 2.016 to 4.334 GHz.

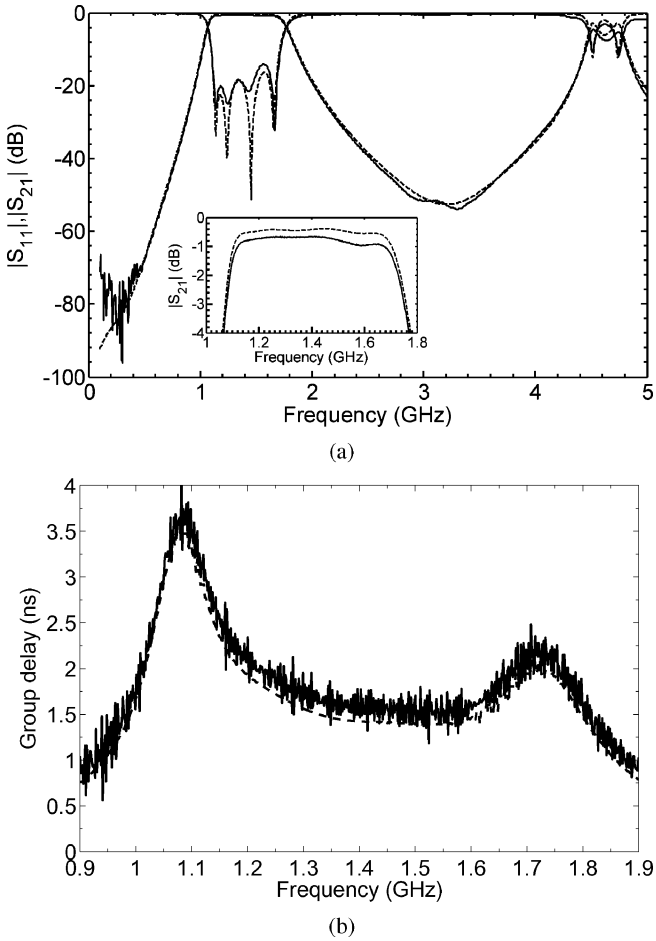

Fig. 23. Simulated (dashed line) and measured (solid line) results of the $\lambda/4$ hairpin filter. (a) Scattering parameters. (b) Passband group delay.

IV. Conclusion

Two types of enhanced coupling structures for parallel coupled microstrip lines have been presented. The coupling strength can be easily varied by adjusting the size of the ground-plane aperture and the width of inserted signal strips. This allows the relaxation of fabrication tolerances since strict dimensions are avoided. The proposed structures are easily fabricated on a single-layer substrate by the conventional PCB process. A novel 3-dB directional coupler and a four-pole $\lambda/4$ parallel-coupled filter with a 40% bandwidth were realized using the proposed coupled-line structures. Moreover, a four-pole $\lambda/4$ hairpin filter with a 37% bandwidth was constructed to demonstrate their convenient applications in the conventional resonator to enhance the coupling between adjacent resonators. These three examples prove that the proposed two structures have successfully solved the coupling strength problem of conventional parallel coupled microstrip lines and are easily applied in many resonator configurations.

References

[1] J. Lange, "Interdigitated stripline quadrature hybrid," *IEEE Trans. Microw. Theory Tech.*, vol. MTT-17, no. 12, pp. 1150–1151, Dec. 1969.

[2] R. Waugh and D. LaCombe, "Unfolding the Lange coupler," *IEEE Trans. Microw. Theory Tech.*, vol. MTT-20, no. 11, pp. 777–779, Nov. 1972.

[3] D. M. Pozar, *Microwave Engineering*, 3rd ed. New York: Wiley, 2005.

[4] Y. Konishi, I. Awai, Y. Fukuoka, and M. Nakajima, "A directional coupler of a vertically installed planar circuit structure," *IEEE Trans. Microw. Theory Tech.*, vol. 36, no. 6, pp. 1057–1063, Jun. 1988.
[5] H. C. Chen and C. Y. Chang, "Modified vertically installed planar couplers for ultrabroadband multisection quadrature hybrid," *IEEE Microw. Wireless Compon. Lett.*, vol. 16, no. 8, pp. 446–448, Aug. 2006.
[6] T. Tanaka, K. Tsunoda, and M. Aikawa, "Slot-coupled directional couplers between double-sided substrate microstrip lines and their applications," *IEEE Trans. Microw. Theory Tech.*, vol. 36, no. 12, pp. 1752–1757, Dec. 1988.
[7] F. Tefiku, E. Yamashita, and J. Funada, "Novel directional couplers using broadside-coupled coplanar waveguides for double-sided printed antennas," *IEEE Trans. Microw. Theory Tech.*, vol. 44, no. 2, pp. 275–282, Feb. 1996.
[8] A. Sawicki and K. Sachse, "Novel coupled-line conductor-backed coplanar and microstrip directional couplers for PCB and LTCC applications," *IEEE Trans. Microw. Theory Tech.*, vol. 51, no. 6, pp. 1743–1751, Jun. 2003.
[9] K. S. Chin, M. C. Ma, Y. P. Chen, and Y. C. Chiang, "Closed-form equations of conventional microstrip couplers applied to design couplers and filters constructed with floating-plate overlay," *IEEE Trans. Microw. Theory Tech.*, vol. 56, no. 5, pp. 1172–1179, May 2008.
[10] J. C. Chiu, C. M. Lin, and Y. H. Wang, "A 3-dB quadrature coupler suitable for PCB circuit design," *IEEE Trans. Microw. Theory Tech.*, vol. 54, no. 9, pp. 3521–3525, Sep. 2006.
[11] C. P. Chang, J. C. Chiu, H. Y. Chiu, and Y. H. Wang, "A 3-dB quadrature coupler using broadside-coupled coplanar waveguides," *IEEE Microw. Wireless Compon. Lett.*, vol. 18, no. 3, pp. 191–193, Mar. 2008.
[12] L. Zhu and K. Wu, "Multilayered coupled-microstrip lines technique with aperture compensation for innovative planar filter design," in *Proc. Asia–Pacific Microw. Conf.*, Singapore, Nov. 1999, vol. 2, pp. 303–306.
[13] S. Im, C. Seo, J. Kim, Y. Kim, and N. Kim, "Improvement of microstrip open loop resonator filter using aperture," in *IEEE MTT-S Int. Microw. Symp. Dig.*, Jun. 2002, vol. 3, pp. 1801–1804.
[14] M. D. C. Velazquez-Ahumada, J. Martel, and F. Medina, "Parallel coupled microstrip filters with ground-plane aperture for spurious band suppression and enhanced coupling," *IEEE Trans. Microw. Theory Tech.*, vol. 52, no. 3, pp. 1082–1086, Mar. 2004.
[15] P. H. Deng, C. H. Wang, and C. H. Chen, "Novel broadside-coupled bandpass filters using both microstrip and coplanar-waveguide resonators," *IEEE Trans. Microw. Theory Tech.*, vol. 54, no. 10, pp. 3746–3750, Oct. 2006.
[16] T. N. Kuo, S. C. Lin, C. H. Wang, and C. H. Chen, "Compact bandpass filters based on dual-plane microstrip/coplanar-waveguide structure with quarter-wavelength resonators," *IEEE Microw. Wireless Compon. Lett.*, vol. 17, no. 3, pp. 178–180, Mar. 2007.
[17] M. K. Mandal and S. Sanyal, "Compact wideband bandpass filter using microstrip to slotline broadside-coupling," *IEEE Microw. Wireless Compon. Lett.*, vol. 17, no. 9, pp. 640–642, Sep. 2007.
[18] M. Tran and C. Nguyen, "Modified broadside-coupled microstrip lines suitable for MIC and MMIC applications and a new class of broadside-coupled bandpass filters," *IEEE Trans. Microw. Theory Tech.*, vol. 41, no. 8, pp. 1336–1342, Aug. 1993.
[19] J. T. Kuo and E. Shih, "Wideband bandpass filter design with three-line microstrip structures," in *IEEE MTT-S Int. Microw. Symp. Dig.*, May 2001, vol. 3, pp. 1593–1596.
[20] W. Menzel, L. Zhu, K. Wu, and F. Bogelsack, "On the design of novel compact broadband planar filters," *IEEE Trans. Microw. Theory Tech.*, vol. 51, no. 2, pp. 364–370, Feb. 2003.
[21] Y. C. Chiou, J. T. Kuo, and E. Cheng, "Broadband quasi-Chebyshev bandpass filters with multimode stepped-impedance resonators (SIRs)," *IEEE Trans. Microw. Theory Tech.*, vol. 54, no. 8, pp. 3352–3358, Aug. 2006.
[22] T. N. Kuo, S. C. Lin, C. H. Wang, and C. H. Chen, "New coupling scheme for microstrip bandpass filters with quarter-wavelength resonators," *IEEE Trans. Microw. Theory Tech.*, vol. 56, no. 12, pp. 2930–2935, Dec. 2008.
[23] C. H. Liang and C. Y. Chang, "Compact wideband bandpass filters using stepped-impedance resonators and interdigital coupling structures," *IEEE Microw. Wireless Compon. Lett.*, vol. 19, no. 9, pp. 551–553, Sep. 2009.
[24] *"Em User's Manual,"* Sonnet Softw., Liverpool, NY, 2004.
[25] *Reference Guide Microwave Office*. El Segundo, CA: AWR, 2003.
[26] M. D. C. Velazquez-Ahumada, J. Martel, and F. Medina, "Parallel coupled microstrip filters with floating ground-plane conductor for spurious-band suppression," *IEEE Trans. Microw. Theory Tech.*, vol. 53, no. 5, pp. 1823–1828, May 2005.
[27] Y. S. Lin, C. H. Wang, C. H. Wu, and C. H. Chen, "Novel compact parallel-coupled microstrip bandpass filters with lumped-element K-inverters," *IEEE Trans. Microw. Theory Tech.*, vol. 53, no. 7, pp. 2324–2328, Jul. 2005.
[28] J. S. Hong and M. J. Lancaster, *Microstrip Filters for RF/Microwave Applications*. New York: Wiley, 2001.

Cheng-Hsien Liang was born in Kaohsiung, Taiwan, on November 5, 1982. He received the B.S. and M.S. degrees in communication engineering from National Chiao-Tung University, Hsinchu, Taiwan, in 2005 and 2007, respectively, and is currently working toward the Ph.D. degree in communication engineering at National Chiao-Tung University.

His research interests include the analysis and design of microwave and millimeter-wave circuits.

Wei-Shin Chang was born in Taipei, Taiwan, on September 15, 1986. She received the B.S. degree in physics from National Taiwan Normal University, Taipei, Taiwan, in 2009 and is currently working toward the Ph.D. degree in communication engineering at National Chiao-Tung University, Hsinchu, Taiwan.

Her research interests include the analysis and design of periodic structures and microwave circuits.

Chi-Yang Chang (M'95) was born in Taipei, Taiwan, on December 20, 1954. He received the B.S. degree in physics and M.S. degree in electrical engineering from National Taiwan University, Taipei, Taiwan, in 1977 and 1982, respectively, and the Ph.D. degree in electrical engineering from The University of Texas at Austin, in 1990.

From 1990 to 1995, he was an Associate Researcher with the Chung-Shan Institute of Science and Technology (CSIST), where he was in charge of development of uniplanar circuits, ultra-broadband circuits, and millimeter-wave planar circuits. In 1995, he joined the faculty of the Department of Communication Engineering (renamed the Department of Electrical Engineering in 2009), National Chiao-Tung University, Hsinchu, Taiwan, as an Associate Professor, and became a Professor in 2002. His research interests include microwave and millimeter-wave passive and active circuit design, planar miniaturized filter design, and MMIC design.